Acta Biochim Biophys Sin, 2015, 47(9), 680–686
doi: 10.1093/abbs/gmv066
Advance Access Publication Date: 22 July 2015
Original Article

Original Article

In vitro effects of phenytoin and DAPT on MDA-MB-231 breast cancer cells

Canan Cakir Aktas[1], N. Dilara Zeybek[2], and A. Kevser Piskin[1,*]

[1]Department of Medical Biochemistry, Faculty of Medicine, Hacettepe University, Ankara 06100, Turkey, and [2]Department of Histology and Embryology, Faculty of Medicine, Hacettepe University, Ankara 06100, Turkey

*Correspondence address. Tel: +90-312-3051652; Fax: +90-312-3245885; E-mail: akpiskin@gmail.com

Received 23 February 2015; Accepted 24 April 2015

Abstract

Voltage-gated sodium channel (VGSC) activity enhances cell behaviors related to metastasis, such as motility, invasion, and oncogene expression. Neonatal alternative splice form of Nav1.5 isoform is expressed in metastatic breast cancers. Furthermore, aberrant Notch signaling pathway can induce oncogenesis and may promote the progression of breast cancers. In this study, we aimed to analyze the effect of the nNav1.5 inhibitor phenytoin and Notch signal inhibitor *N*-[*N*-(3,5-difluorophenacetyl)-L-alanyl]-S-phenylglycine-*t*-butyl ester (DAPT) on triple negative breast cancer cell line (MDA-MB-231) via inhibition of nNav1.5 VGSC activity and Notch signaling, respectively. In order to determine the individual and combined effects of these inhibitors, the 4-[3-(4-iyodophenyl)-2-(4-nitrophenyl)-2H-5-tetrazolio]-1,3-benzene disulfonate (WST-1) test, wound healing assay, and zymography were performed to detect the proliferation, lateral motility, and matrix metalloproteinase-9 (MMP9) activity, respectively. The expressions of *nNav1.5*, *Notch4*, *MMP9*, and tissue inhibitor of metalloproteinases-1 (*TIMP1*) were also detected by quantitative real-time reverse transcriptase–polymerase chain reaction. DAPT caused an antiproliferative effect when the doses were higher than 10 μM, whereas phenytoin showed no inhibitory action either alone or in combination with DAPT on the MDA-MB-231 cells. Furthermore, it was found that the lateral motility was inhibited by both inhibitors; however, this inhibitory effect was partially rescued when they were used in combination. Meanwhile, the results showed that the MMP9 activity and the ratio of *MMP9* mRNA to *TIMP1* mRNA were only decreased by DAPT. Thus, we conclude that the combined effect of DAPT and phenytoin is not as beneficial as using DAPT alone on MDA-MB-231 breast cancer cells.

Key words: breast cancer, voltage-gated Na^+ channel, Notch4 receptor, matrix metalloproteinase 9, tissue inhibitor of metalloproteinase 1

Introduction

Globally, invasive breast cancer still perils the life of many women and is a big threat for female longevity. Understanding the mechanism of metastasis and developing effective treatment strategies aiming at cancer metastasis is a major goal. Therefore, molecular mechanisms involved in the metastatic behavior of breast cancer cells are rapidly emerging as critical therapeutic targets [1,2].

Voltage-gated sodium channels (VGSCs) and Notch receptor signaling contribute to metastatic process in many types of carcinomas. Several individual Nav (Nav1.1–1.9) isoforms of VGSCs are functionally expressed in different human cancers [3–6]. In particular, the alternative splice variant of the Nav1.5 isoform, named as Nav1.5 neonatal D1:S3 5′-splice form (nNav1.5), has been found to be expressed in some metastatic cancer cells, especially in highly metastatic MDA-MB-231 breast cancer cells [7–9].

Suppressing the channel activity and expression by chronic blockage of VGSCs provide a dual advantage in any clinical anti-metastatic treatment. Tetrodotoxin (TTX), blocking antibodies, small interfering RNA (siRNA), certain pharmaceutics, and fatty acids could suppress VGSC activity [10]. Inhibition of VGSCs by TTX supresses various

metastatic cell behaviors including lateral motility [11], invasion [12], galvanotaxis [13], transverse migration [14], adhesion [15], endocytic membrane activity [16], vesicular patterning [17], and nitric oxide production [18].

Furthermore, suppression of the channel by RNA interference inhibits VGSC-dependent migration and invasion in MDA-MB-231 human breast cancer cells [7,12]. Some pharmacological agents similar to local anesthetics such as lidocaine or phenytoin, which are anticonvulsants, also inhibit the VGSC-dependent augmentation of endocytic membrane activity in small cell lung cancer cell lines [19]. Phenytoin also inhibits the migration and invasion of metastatic breast cancer cells by targeting the Nav1.5 sodium channel [20].

Another potential molecular target for breast cancer therapy is the Notch receptor system. Notch receptor signaling regulates cell fate determination, proliferation, differentiation, and survival. There are four types of Notch receptors in vertebrates (Notchs 1–4) and at least five ligands belonging to Delta and JAG/Serrate (DSL) families. Notch4 plays a terminal role in mammary tissue development [21,22]. Notch receptor overexpression has been detected in a variety of cancers including breast cancer [23–27]. Aberrant expression of Notch receptor and its pathway components have been implicated with metastatic breast cancer cells [28].

In recent years, there has been a growing interest in the Notch receptor system as a target for breast cancer treatment [1]. In fact, Notch receptor inhibitors are now making their ways to clinical trials [29]. In order to consider the Notch system as an efficient target, its interactions with other pathways that play critical roles in breast cancer must be understood. This understanding may facilitate the selection of optimal compounds for use in combination with Notch inhibitors [23,29–32].

Therefore, we aimed to study the combined and individual effects of the Notch signal inhibitor *N*-[*N*-(3,5-difluorophenacetyl)-L-alanyl]-S-phenylglycine-*t*-butyl ester (DAPT) and the nNav1.5 inhibitor phenytoin on lateral motility, cell proliferation, and matrix metalloproteinase-9 (MMP9) activation in MDA-MB-231 breast cancer cells.

Materials and Methods

Cell culture

The human breast cancer cell line MDA-MB-231 was purchased from American Type Culture Collection (ATCC, Wesel, Germany), and cells were cultured in high-glucose Dulbecco's modified Eagle's medium (Sigma, St Louis, USA) supplemented with 10% heat-inactivated fetal bovine serum (Sigma), 2 mM L-glutamine (Sigma), and 1% antibiotic–antimycotic solution (Sigma) under standard culture conditions (37°C, 100% humidity, and 5% CO_2).

Cell proliferation assay

Cell proliferation was assessed using a colorimetric assay with 4-[3-(4-iodophenyl)-2-(4-nitrophenyl)-2H-5-tetrazolio]-1,3-benzene disulfonate (WST-1) reagent (Roche, Basel, Switzerland). Briefly, MDA-MB-231 cells were seeded in 96-well plates (4×10^4 cells per well) and allowed to adhere overnight. After 24 h, the cells were treated with DAPT (Calbiochem, San Diego, USA), phenytoin (Sigma), or with the combination of these molecules at doses ranging between 0.1 and 500 μM, or vehicle for 24, 48, and 72 h. Then, 10 μl of WST-1 was added and incubated for 4 h at 37°C. The absorption of cells was measured at 420–600 nm using a microplate reader (Spectra Max, Molecular Devices, Sunnyvale, USA). The solvents of phenytoin and DAPT, namely, sodium hydroxide and dimethyl sulfoxide, were applied as background controls.

Cell motility assay

The lateral motility of MDA-MB-231 cells was examined by performing the wound healing assay [33]. The cells (5×10^5 cells per well) were seeded in six-well plates. After 24 h, three wounds were produced in each well using a P1000 pipette tip. The wells were rinsed once with fresh medium, and wound widths were recorded under an inverted microscope (Leica, Wetzlar, Germany). These cells were treated with phenytoin, DAPT, or the combination of DAPT and phenytoin at doses of 7, 70, and 700 μM and incubated for 24 h. Then the same wound areas were re-measured. Motility was expressed as per cent decrease of width in wound areas compared with untreated cells.

Quantitative real-time polymerase chain reaction

The expression levels of *Notch4* (*nNav1.5*), *MMP9*, and tissue inhibitor of metalloproteinases-1 (*TIMP1*) were analyzed by quantitative real-time polymerase chain reaction (qRT-PCR) using Rotor Gene Q apparatus (Qiagen, Hilden, Germany). Total RNA was isolated from MDA-MB-231 cells by using RNAeasy Mini kit (Qiagen). The first strand of cDNA was reverse transcribed from 2.5 μg of total RNA using RT^2 First Strand kit (Qiagen), according to the manufacturer's instruction. qRT-PCR was performed using SYBR Green PCR Master Mix (Qiagen). The primers used for PCR are listed in **Table 1**. The amplification reaction was performed as follows: denaturation at 94°C for 15 s, followed by annealing at 55°C for 30 s, and extension at 72°C for 30 s. Data normalization was performed by using the threshold cycle value (Ct) of the human *GAPDH* gene (Ct−Ct GAPDH = ΔCt). ΔCt values for each sample were then normalized to control samples. Results were expressed as a fold change in mRNA expression relative to control samples [34].

Gelatin zymography

Gelatin zymography assay was performed to detect the activity of MMP9, as described elsewhere [35]. MDA-MB-231 cells were treated with DAPT, phenytoin, or the combination at doses of 7, 70, and 700 μM. After 24 h, the culture media were collected and applied to 10% non-reducing sodium dodecyl sulfate–polyacrylamide gel containing 0.1% gelatin (Sigma). Proteins were separated by running at 125 mV for 1.5 h. Gels were renatured using 2.5% Triton X-100. Then, they were incubated in developing buffer at 37°C for 15 h. Bands were detected after staining with Coomassie Blue R-250 and quantified by Image Quant TL software.

Table 1. Primers used in qRT-PCR

Genes	Primers
nNav1.5	Forward: 5′-CATCCTCACCAACTGCGTGT-3′
	Reverse: 5′-CCTAGTTTTTCTGATACA-3′
Notch4	Forward: 5′-AGTCCAGGCCTTGCCAGAACG-3′
	Reverse: 5′-GTAGAAGGCATTGGCCAGAGAG-3′
MMP9	Forward: 5′-GACGAGGGCCTGGAGTGT-3′
	Reverse: 5′-TGTGCTGTAGGAAGCTCATCTC-3′
TIMP1	Forward: 5′-ACCCCTGGAGCACGGCT-3′
	Reverse: 5′-CCCACCTTCCAAGTTAGTGACA-3′
GAPDH	Forward: 5′-CGGAGTCAACGGATTTGGTCGTAT-3′
	Reverse: 5′-AGCCTTCTCCAT GGTGGTGAAGAC-3′

Statistical analysis

All quantitative data were presented as the mean ± standard deviation (SD) from three independent experiments. Statistical analysis was conducted using SPSS software version 15.0. Multiple comparisons between data sets were performed by analysis of variance (ANOVA), followed by Tukey's *post hoc* test. $P < 0.05$ was considered significant difference.

Results

Phenytoin decreases the antiproliferative effect of DAPT

DAPT caused a dose-dependent antiproliferative effect on MDA-MB-231 cells at 24 h with doses higher than 10 μM having an IC_{50} value of 690 μM (**Fig. 1**). The antiproliferative effect of DAPT was decreased when the treatment time was increased to 48 or 72 h, which had the IC_{50} values of 973 and 880 μM, respectively (data not shown). Next, we tested whether a combination of a specific gamma-secretase inhibitor DAPT with a specific VGSC inhibitor phenytoin could produce a synergistic effect in inhibiting proliferation. The results indicated that phenytoin did not exert any effect on proliferation, and in fact when combined with equal doses of DAPT (from 0.1 to 500 μM such as 0.1 μM DAPT + 0.1 μM phenytoin, 1 μM DAPT + 1 μM phenytoin, and so forth), phenytoin decreased the antiproliferative effect of DAPT on MDA-MB-231 cells (**Fig. 1**).

DAPT and phenytoin single treatment are more effective in inhibiting lateral motility when compared with combined treatment

The inhibitory effects of phenytoin, DAPT, and phenytoin–DAPT combination on lateral motility of MDA-MB-231 cells were tested by a 24 h wound healing assay (**Fig. 2**). Phenytoin inhibited cell motility by 20% ± 1.4% at a dose of 7 μM. The effect was more pronounced at doses of 70 and 700 μM, with an inhibition up to 87% ± 1.3% ($P < 0.05$ and $n = 3$; **Fig. 2A,D**). DAPT exerted an inhibitory action on the lateral motility of MDA-MB-231 cells in a dose-dependent manner. Inhibition ratios were 49% ± 1.4%, 61% ± 1.3%, and 82% ± 1.3% at doses of 7, 70, and 700 μM, respectively ($P < 0.05$ and $n = 3$; **Fig. 2B,D**).

Then, the synergistic inhibitory effect of the combination of DAPT–phenytoin at the same doses (7, 70, and 700 μM) on lateral motility was also examined. When applied together, they reduced the inhibitory effects of each other on the lateral motility (37% ± 1.4%, 49% ± 1.3% and 52% ± 1.3%, respectively, $P < 0.05$ and $n = 3$; **Fig. 2C,D**). Our findings demonstrated that the single treatment of DAPT and phenytoin was more effective when compared with the combined treatment.

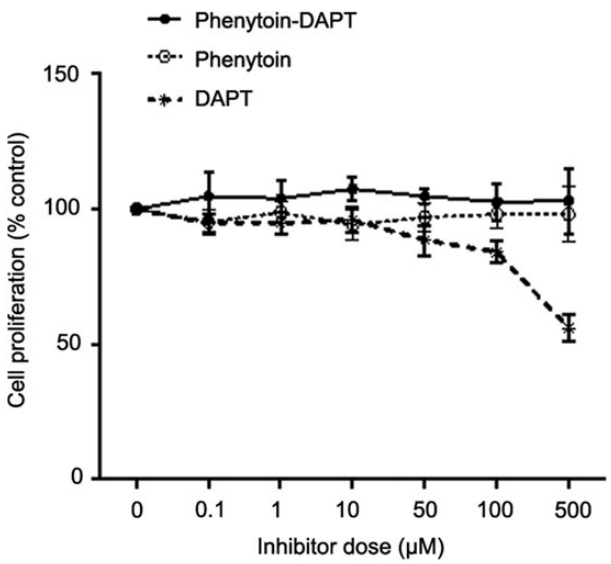

Figure 1. Effects of phenytoin, DAPT, and their combination on the proliferation of MDA-MB-231 cells Cells were treated with different doses of phenytoin, DAPT, and their combinations. The inhibitors were applied at equal doses (0.1–500 μM) either alone or combined. Cell proliferation was assessed by WST-1. Data represent the average percentages of three independent experiments (mean ± SD).

Phenytoin changes the effect of DAPT on the mRNA levels of *nNav1.5, Notch4, MMP9,* and *TIMP1*

A significant decrease was detected in the mRNA levels of *nNav1.5* at all concentrations of phenytoin and DAPT, except at 70 μM phenytoin alone. Treatment with 70 μM phenytoin alone led to 61% ± 0.01% increase in the mRNA levels of *nNav1.5*, but combined treatment with 7 μM DAPT resulted in a decrease by 61% ± 0.08%. This decrease was 70% and 72% for 70 μM phenytoin + 70 μM DAPT and 70 μM phenytoin + 700 μM DAPT, respectively. DAPT at the single doses of 7, 70, and 700 μM decreased the *nNav1.5* expression by 39% ± 0.08%, 77% ± 0.17%, and 62% ± 0.16% ($P < 0.05$ and $n = 6$; **Fig. 3A**), respectively. Interestingly, application of DAPT alone or in combination with phenytoin decreased the mRNA levels of *nNav1.5*.

The effects of DAPT, phenytoin, and the combination of DAPT–phenytoin on the mRNA levels of *MMP9* and *TIMP1* were further examined. The expression levels of *MMP9* decreased by 28% ± 0.2%, whereas the *TIMP1* expression levels increased by about 2.7-fold after 24 h treatment with 70 μM phenytoin + 700 μM DAPT. With 700 μM DAPT alone, the *TIMP1* expression significantly increased by about 6.3-fold when compared with the untreated cells ($P < 0.05$ and $n = 6$; **Fig. 3B**).

Diminished activation of MMP9 by DAPT increases in combination with phenytoin

In our study, the activity of MMP9 decreased by 46.8% ± 3.9% ($P < 0.05$ and $n = 3$; **Fig. 4**) in MDA-MB-231 cells treated with 700 μM DAPT. In contrast, the MMP9 activity increased by 19% ± 2.4% and 21% ± 1.7% in MDA-MB-231 cells treated with 70 μM phenytoin and 70 μM phenytoin+7 μM DAPT, respectively, compared with the untreated cells for 24 h ($P < 0.05$ and $n = 3$; **Fig. 4**).

Activity of MMP9 proteins and its mRNA levels were directly correlated. Although 700 μM DAPT decreased MMP9 activity by 46.8%, this effect was reduced to 16.2% by addition of 70 μM phenytoin. Phenytoin decreased the reducing effect of DAPT on the *MMP9*/*TIPM1* mRNA ratio. The reduction of this ratio by 700 μM DAPT (86%) was 74% when 70 μM phenytoin was added ($P < 0.05$ and $n = 3$; **Fig. 3C**). But, phenytoin alone or in combination with DAPT did not decrease the MMP9 activity.

Discussion

Several molecular signals play crucial roles in the metastatic process of breast cancer. Phenytoin decreases parameters related to metastatic ability such as invasion and motility [20]. Notch receptors contribute to the invasiveness of metastatic breast cancer cells [36,37]. The effects of phenytoin and DAPT were investigated on triple negative breast cancer cell line (MDA-MB-231) via inhibition of VGSC activity and Notch signaling, respectively. In our study, DAPT caused an anti-

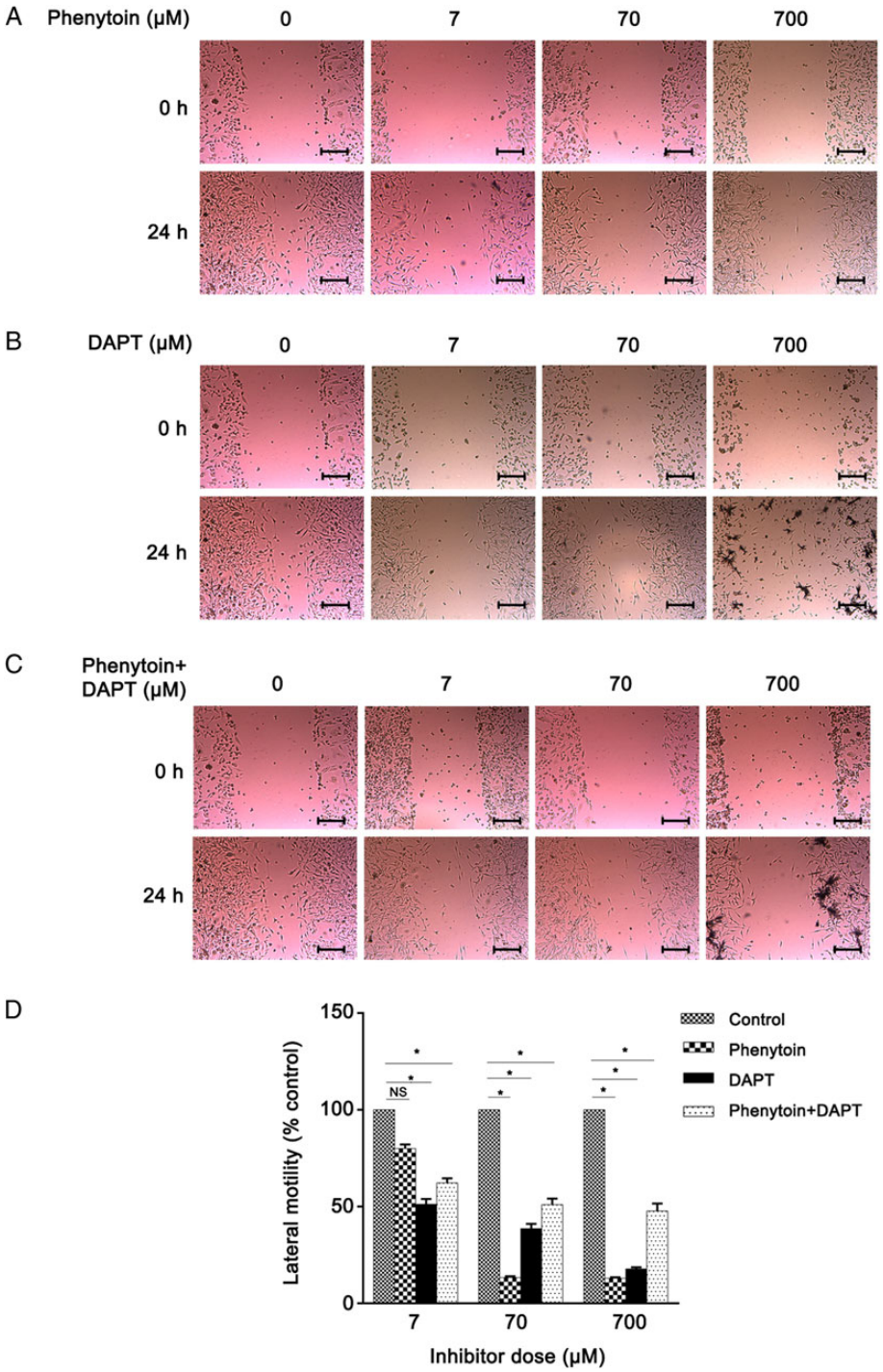

Figure 2. Effects of phenytoin (A), DAPT (B), and their combination (C) on the lateral migration of MDA-MB-231 cells Inhibitors were applied equally at doses of 7, 70, and 700 μM either alone or in combination. Scale bar represents 250 μm. The wounds were generated by a pipette tip. The width of the wound area in each sample was compared with that of its zero hour counterpart. The percent inhibition of lateral motility is given (D). Data represent percent inhibition when compared with untreated control cells and given as mean of three experiments (mean ± SD). *$P < 0.05$. NS, not significant.

proliferative effect on MDA-MB-231 cells in a dose-dependent manner over a 24 h period at doses higher than 10 μM. It was reported that DAPT and other gamma-secretase inhibitors such as L-685,458 have no anti-proliferative effect at lower doses [38], which supports our findings. VGSCs do not play any role in cellular proliferation [3]. Furthermore, inhibition of VGSCs by phenytoin, the anti-proliferative effect of DAPT, was decreased. This suggests that phenytoin exerts an antagonistic effect with DAPT on the proliferation of MDA-MB231 cells. Phenytoin which suppresses VGSCs acts on the metastatic properties of the MDA-MB231 cells [20]. One of the metastatic properties, namely, lateral motility, was analyzed by wound healing test. It was found that both DAPT and phenytoin decreased

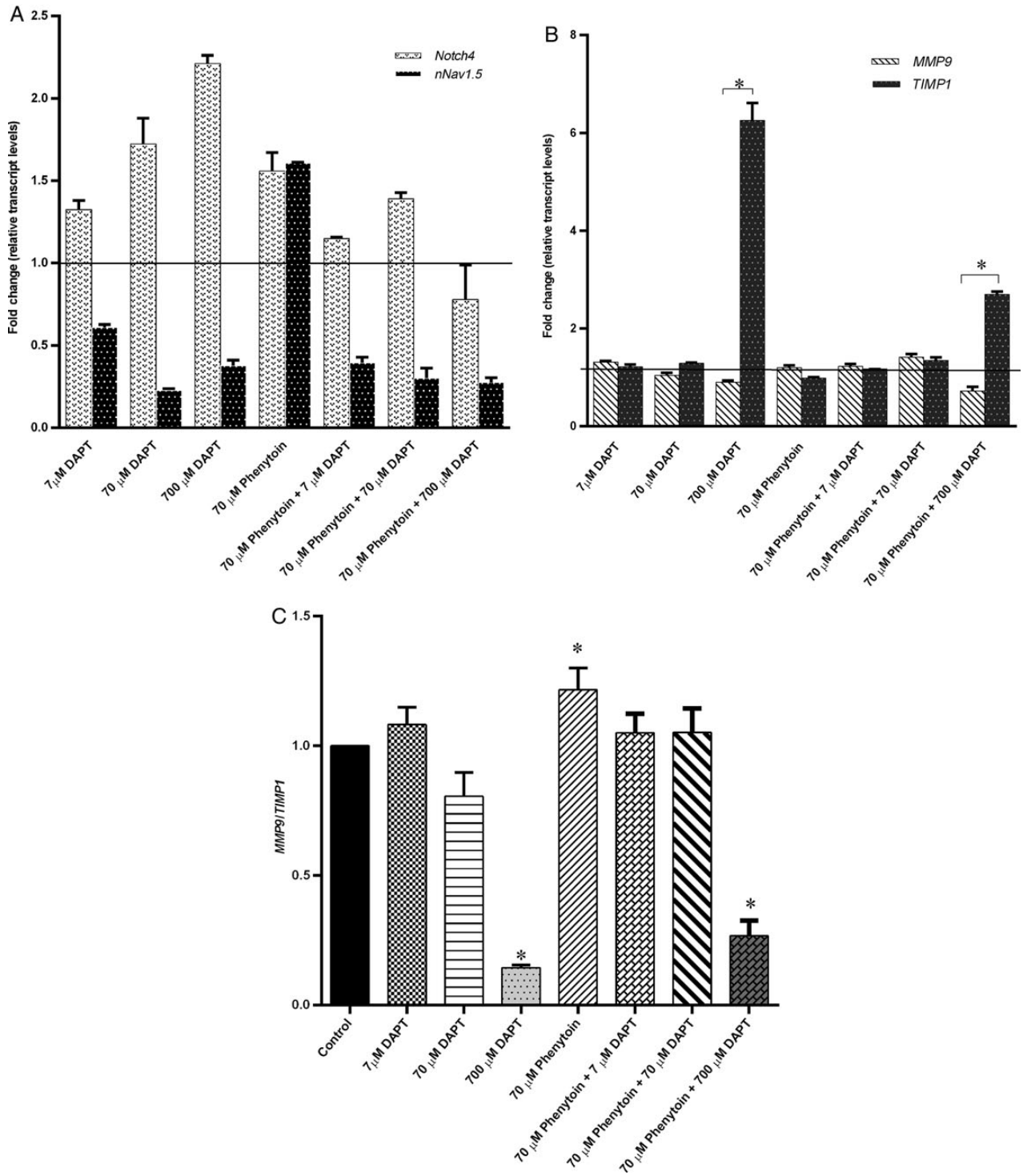

Figure 3. Average expression profiles of *nNav1.5* and *Notch4* (A) and *MMP9* and *TIMP1* (B) and the ratio of *MMP9/TIMP1* relative transcript levels (C) Each experiment was conducted in triplicate, and data were normalized to the expression of *GAPDH* and calibrated to the expression levels in untreated cells. MDA-MB-231 cells were treated with 7 μM DAPT, 70 μM DAPT, 700 μM DAPT, 70 μM phenytoin, 70 μM phenytoin + 7 μM DAPT, 70 μM phenytoin+70 μM DAPT, and 70 μM phenytoin+700 μM DAPT for 24 h. Fold changes below 0.5 and above 1.3 are considered as significant with $P < 0.05$ as determined by ANOVA with Tukey's HSD *post hoc*. Results are presented as the mean ± SD.

lateral motility of these cells. Recently, it was reported that phenytoin decreased the cell migration of rat prostate cancer cells [11]. Similarly, it was previously demonstrated that treatment of MDA-MB-231 cells with 50 and 200 μM phenytoin resulted in 27.3% ± 1.9% and 37.2% ± 1.8% decrease in motility, respectively [20]. Our findings are also consistent with Chigurupati *et al.* [39], who found that inhibition of Notch signaling by using gamma-secretase inhibitors resulted in impaired wound healing process in keratinocytes or fibroblasts.

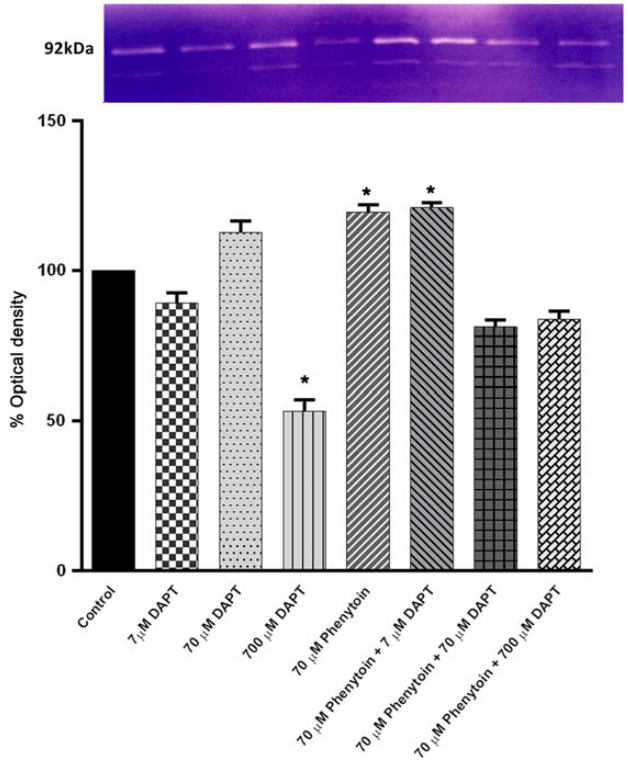

Figure 4. Zymographic analysis of MMP9 activity in MDA-MB-231 cells The graph shows the inverted densitometric analysis of bands. MDA-MB-231 cells were treated with 7 μM DAPT, 70 μM DAPT, 700 μM DAPT, 70 μM phenytoin, 70 μM phenytoin + 7 μM DAPT, 70 μM phenytoin+70 μM DAPT, and 70 μM phenytoin + 700 μM DAPT for 24 h. Band densities of treated cell samples were compared with those of control cells. Results are presented as the mean ± SD. *$P < 0.05$.

Furthermore, wound healing capacity of cells transfected by siRNA duplexes targeting either Notch4 or Hes1 was impaired by 22.5% ± 2.1% and 27.0% ± 1.3% when compared with scramble control, respectively [40]. Some pharmacological agents may affect gene expression indirectly with a mechanism yet to be determined. Therefore, we tested DAPT and phenytoin for their possible action. Phenytoin does not decrease mRNA expression levels of *nNav1.5*. Although previous reports have suggested that phenytoin suppresses the nNav1.5 channel activity [20], they did not show the effect of phenytoin on the *nNav1.5* mRNA expression level. In cancer cells, the expression of VGSCs is regulated mostly by positive feedback mechanisms contrary to normal cells. For this reason, more effective inhibitors that decrease mRNA levels of the channel may suppress metastatic behaviors of cancer cells. Therefore, further investigation will be required to design new agents that target at channel activity and functional channel expression or to determine which chemicals suppress both VGSC mRNA levels and activity. Interestingly, application of DAPT alone or together with phenytoin decreased the mRNA levels of *nNav1.5*. This decline may stem from the fact that gamma-secretase inhibitors have several substrates besides gamma secretase, which is one of the drawbacks of using them. A previous study indicated that the β-subunit of VGSCs is a substrate of gamma-secretase inhibitors [40]. Moreover, inhibition of Notch signal pathway via DAPT increased *Notch4* mRNA levels. This may be a response to signal inhibition. Remarkably, the expression ratio of *MMP9* to *TIMP1* was decreased by the application of both agents. This is consistent with our findings using gelatin zymography technique, which may demonstrate the decreased protein level of MMP9. Further studies should be carried out to confirm these expression changes either by Northern or western blotting. Enzymes that mediate invasion and metastasis of tumor cells include MMPs, serine proteases, cysteine proteases, and aspartyl proteinases. Among these, MMPs are Zn^{2+}-dependent peptides that can degrade extracellular matrix. It was reported that MMP9 is activated in breast cancer, and high expression of MMP9 is responsible for metastasis of breast cancer cells [41,42]. They are secreted in a latent form as pro-MMPs. Activation of MMPs is regulated by activators and inhibitors [43]. The balance between MMPs and their inhibitors (TIMPs) is crucial for the maintenance of extracellular matrix. In most human cancers, an increase in *MMP* gene activity was also reported [44]. The inhibitory effect of phenytoin on an extracellular matrix regulator, namely, collagenase, has been reported in patients with epidermolysis bullosa [45]. However, we have found that phenytoin increased the gelatinase activity of MMP9, which is another regulator in the extracellular matrix.

In conclusion, the results of this study indicate that DAPT decreases cell proliferation as well as lateral motility, MMP9 activity, and proportional gene expression of *MMP9* to *TIMP1 in* MDA-MB-231 cells. Moreover, it significantly decreases the mRNA levels of *nNav1.5*. This supports the idea that the Notch signaling system is a suitable target in the treatment of metastatic breast cancer cells. In contrast, the combined use of DAPT and phenytoin reduces these effects because of interactions of these inhibitors with mechanisms yet to be determined. It is concluded that DAPT and phenytoin do not act synergistically on MDA-MB-231 breast cancer cells. Thus, the combined use of DAPT with phenytoin is not as beneficial as single DAPT application.

References

1. Al-Hussaini H, Subramanyam D, Reedijk M, Sridhar SS. Notch signaling pathway as a therapeutic target in breast cancer. *Mol Cancer Ther* 2010, 10: 9–15.
2. den Hollander P, Savage MI, Brown PH. Targeted therapy for breast cancer prevention. *Front Oncol* 2013, 3: 250.
3. Fraser SP, Diss JK, Mycielska ME, Pan H, Yamaci RF, Pani F, Siwy Z, *et al.* Voltage-gated sodium channel expression and potentiation of human breast cancer metastasis. *Clin Cancer Res* 2005, 11: 5381–5389.
4. Fraser SP, Diss JK, Lloyd LJ, Pani F, Chioni AM, George AJ, Djamgoz MB. T-lymphocyte invasiveness: control by voltage-gated Na^+ channel activity. *FEBS Lett* 2004, 569: 191–194.
5. Grimes JA, Djamgoz MB. Electrophysiological characterization of voltage gated Na^+ current expressed in the highly metastatic Mat-LyLu cell line of rat prostate cancer. *J Cell Physiol* 1998, 175: 50–58.
6. Roger S, Rollin J, Barascu A, Besson P, Raynal PI, Iochmann S, Lei M, *et al.* Voltage-gated sodium channels potentiate the invasive capacities of human non-small-cell lung cancer cell lines. *Int J Biochem Cell Biol* 2007, 39: 774–786.
7. Brackenbury WJ, Chioni AM, Diss JK, Djamgoz MB. The neonatal splice variant of Nav1.5 potentiates *in vitro* invasive behaviour of MDA-MB-231 human breast cancer cells. *Breast Cancer Res Treat* 2007, 101: 149–160.
8. Chioni AM, Fraser SP, Pani F, Foran P, Wilkin GP, Diss JK, Djamgoz MB. A novel polyclonal antibody specific for the Na(v)1.5 voltage-gated Na(+) channel 'neonatal' splice form. *J Neurosci Methods* 2005, 147: 88–98.
9. Gao R, Wang J, Shen Y, Lei M, Wang Z. Functional expression of voltage gated sodium channels Nav1.5 in human breast cancer cell line MDA-MB-231. *J Med Sci* 2009, 29: 64–67.
10. Onkal R, Djamgoz MB. Molecular pharmacology of voltage-gated sodium channel expression in metastatic disease: clinical potential of neonatal Nav1.5 in breast cancer. *Eur J Pharmacol* 2009, 625: 206–219.

11. Fraser SP, Salvador V, Manning EA, Mizal J, Altun S, Raza M, Berridge RJ, *et al*. Contribution of functional voltage-gated Na^+ channel expression to cell behaviors involved in the metastatic cascade in rat prostate cancer: I. Lateral motility. *J Cell Physiol* 2003, 195: 479–487.
12. Gillet L, Roger S, Besson P, Lecaille F, Gore J, Bougnoux P, Lalmanach G, *et al*. Voltage-gated sodium channel activity promotes cysteine cathepsin-dependent invasiveness and colony growth of human cancer cells. *J Biol Chem* 2009, 284: 8680–8691.
13. Djamgoz MB, Mycielska M, Madeja Z, Fraser SP, Korohoda W. Directional movement of rat prostate cancer cells in direct-current electric field: involvement of voltage gated Na^+ channel activity. *J Cell Sci* 2001, 114: 2697–2705.
14. Roger S, Besson P, Le Guennec JY. Involvement of a novel fast inward sodium current in the invasion capacity of a breast cancer cell line. *Biochim Biophys Acta* 2003, 1616: 107–111.
15. Palmer CP, Mycielska ME, Burcu H, Osman K, Collins T, Beckerman R, Perret R, *et al*. Single cell adhesion measuring apparatus (SCAMA): application to cancer cell lines of different metastatic potential and voltage-gated Na^+ channel expression. *Eur Biophys J* 2008, 37: 359–368.
16. Nakajima T, Kubota N, Tsutsumi T, Oguri A, Imuta H, Jo T, Oonuma H, *et al*. Eicosapentaenoic acid inhibits voltage-gated sodium channels and invasiveness in prostate cancer cells. *Br J Pharmacol* 2009, 156: 420–431.
17. Krasowska M, Grzywna ZJ, Mycielska ME, Djamgoz MB. Patterning of endocytic vesicles and its control by voltage-gated Na^+ channel activity in rat prostate cancer cells: fractal analyses. *Eur Biophys J* 2004, 33: 535–542.
18. Williams EL, Djamgoz MB. Nitric oxide and metastatic cell behaviour. *Bio Essays* 2005, 27: 1228–1238.
19. Onganer PU, Djamgoz MB. Small-cell lung cancer (human): potentiation of endocytic membrane activity by voltage-gated Na^+ channel expression *in vitro*. *J Membr Biol* 2005, 204: 67–75.
20. Yang M, Kozminski DJ, Wold LA, Modak R, Calhoun JD, Isom LL, Brackenbury WJ. Therapeutic potential for phenytoin: targeting Nav1.5 sodium channels to reduce migration and invasion in metastatic breast cancer. *Breast Cancer Res Treat* 2012, 134: 603–615.
21. Brennan K, Clarke RB. Combining notch inhibition with current therapies for breast cancer treatment. *Ther Adv Med Oncol* 2013, 5: 17–24.
22. Harrison H, Farnie G, Howell SJ, Rock RE, Stylianou S, Brennan KR, Bundred NJ, *et al*. Regulation of breast cancer stem cell activity by signaling through the Notch4 receptor. *Cancer Res* 2010, 70: 709–718.
23. Callahan R, Egan SE. Notch signaling in mammary development and oncogenesis. *J Mammary Gland Biol Neoplasia* 2004, 9: 145–163.
24. Gray GE, Mann RS, Mitsiadis E, Henrique D, Carcangiu ML, Banks A, Leiman J, *et al*. Human ligands of the notch receptor. *Am J Pathol* 1999, 154: 785–794.
25. Miyamoto Y, Maitra A, Ghosh B, Zechner U, Argani P, Iacobuzio-Donahue CA, Sriuranpong V, *et al*. Notch mediates TGF alpha-induced changes in epithelial differentiation during pancreatic tumorigenesis. *Cancer Cell* 2003, 3: 565–576.
26. Nickoloff BJ, Osborne BA, Miele L. Notch signaling as a therapeutic target in cancer: a new approach to the development of cell fate modifying agents. *Oncogene* 2003, 22: 6598–6608.
27. Purow BW, Haque RM, Noel MW, Su Q, Burdick MJ, Lee J, Sundaresan T, *et al*. Expression of Notch-1 and its ligands, delta-like-1 and jagged-1, is critical for glioma cell survival and proliferation. *Cancer Res* 2005, 65: 2353–2363.
28. Stylianou S, Clarke RB, Brennan K. Aberrant activation of notch signaling in human breast cancer. *Cancer Res* 2006, 66: 1517–1525.
29. Guo S, Liu M, Gonzalez-Perez RR. Role of Notch and its oncogenic signaling crosstalk in breast cancer. *Biochim Biophys Acta* 2011, 1815: 197–213.
30. Haines N, Irvine KD. Glycosylation regulates notch signaling. *Nat Rev Mol Cell Biol* 2003, 4: 786–797.
31. Noseda M, Chang L, McLean G, Grim JE, Clurman BE, Smith LL, Karsan A. Notch activation induces endothelial cell cycle arrest and participates in contact inhibition: role of P21cip1 repression. *Mol Cell Biol* 2004, 24: 8813–8822.
32. Santagata S, Demichelis F, Riva A, Varambally S, Hofer MD, Kutok JL, Kim R, *et al*. Jagged1 expression is associated with prostate cancer metastasis and recurrence. *Cancer Res* 2004, 64: 6854–7657.
33. Scorey N, Fraser SP, Patel P, Pridgeon C, Dallman MJ, Djamgoz MB. Notch signaling and voltage-gated Na^+ channel activity in human prostate cancer cells: independent modulation of *in vitro* motility. *Prostate Cancer Prostatic Dis* 2006, 9: 399–406.
34. Livak KJ, Schmittgen TD. Analysis of relative gene expression data using real time quantitative PCR and the 2(-Delta Delta C(T)) method. *Methods* 2001, 25: 402–408.
35. Toth M, Fridman R. Assessment of gelatinases MMP-2 and MMP-9 by gelatin zymography. *Methods Mol Med* 2001, 57: 163–174.
36. O'Neill CF, Urs S, Cinelli C, Lincoln A, Nadeau RJ, León R, Toher J, *et al*. Notch2 signaling induces apoptosis and inhibits human MDA-MB-231 xenograft growth. *Am J Pathol* 2007, 171: 1023–1036.
37. Wang Z, Banerjee S, Li Y, Rahman KM, Zhang Y, Sarkar FH. Down-regulation of Notch-1 inhibits invasion by inactivation of nuclear factor-kappab, vascular endothelial growth factor, and matrix metalloproteinase-9 in pancreatic cancer cells. *Cancer Res* 2006, 66: 2778–2784.
38. Han J, Ma I, Hendzel M, Allalunis-Turner J. The cytotoxicity of gamma-secretase inhibitor I to breast cancer cells is mediated by proteasome inhibition, not by gamma-secretase inhibition. *Breast Cancer Res* 2009, 11: R57.
39. Chigurupati S, Arumugam TV, Son TG, Lathia JD, Jameel S, Mughal MR, Tang SC, *et al*. Involvement of notch signaling in wound healing. *PloS ONE* 2007, 2: e1167.
40. Kopan R, Ilagan MX. γ-secretase: proteasome of the membrane? *Nat Rev Mol Cell Biol* 2004, 5: 499–504.
41. Kim JJ, Ha AW, Kim HS, Kim WK. Inorganic sulfur reduces the motility and invasion of MDA-MB-231 human breast cancer cells. *Nutr Res Pract* 2011, 5: 375–380.
42. Davies B, Waxman J, Wasan H, Abel P, Williams G, Krausz T, Neal D, *et al*. Levels of matrix metalloproteases in bladder cancer correlate with tumor grade and invasion. *Cancer Res* 1993, 53: 5365–5369.
43. Snoek-van Beurden PA, Von den Hoff JW. Zymographic techniques for the analysis of matrix metalloproteinases and their inhibitors. *Biotechniques* 2005, 38: 73–83.
44. Kim Y, Remagle AG, Chernov AV, Liu H, Shubayev I, Lai C, Dolkas J, *et al*. The MMP-9/TIMP-1 axis controls the status of differentiation and function of myelin-forming Schwann cells in nerve regeneration. *PloS ONE* 2012, 7: 33664.
45. Eisenberg M, Stevens LH, Schofield PJ. Epidermolysis bullosa—new therapeutic approaches. *Australas J Dermatol* 1978, 19: 1–8.